

# Group is better than individual: Exploiting Label Topologies and Label Relations for Joint Multiple Intent Detection and Slot Filling

Bowen Xing<sup>1,2</sup> and Ivor W. Tsang<sup>2,1</sup>

<sup>1</sup>Australian Artificial Intelligence Institute, University of Technology Sydney, Australia

<sup>2</sup>Centre for Frontier Artificial Intelligence Research, A\*STAR, Singapore

bxwing714@gmail.com, ivor.tsang@gmail.com

## Abstract

Recent joint multiple intent detection and slot filling models employ label embeddings to achieve the semantics-label interactions. However, they treat all labels and label embeddings as uncorrelated individuals, ignoring the dependencies among them. Besides, they conduct the decoding for the two tasks independently, without leveraging the correlations between them. Therefore, in this paper, we first construct a Heterogeneous Label Graph (HLG) containing two kinds of topologies: (1) statistical dependencies based on labels' co-occurrence patterns and hierarchies in slot labels; (2) rich relations among the label nodes. Then we propose a novel model termed ReLa-Net. It can capture beneficial correlations among the labels from HLG. The label correlations are leveraged to enhance semantic-label interactions. Moreover, we also propose the label-aware inter-dependent decoding mechanism to further exploit the label correlations for decoding. Experiment results show that our ReLa-Net significantly outperforms previous models. Remarkably, ReLa-Net surpasses the previous best model by over 20% in terms of overall accuracy on MixATIS dataset.

## 1 Introduction

Intent detection and slot filling (Tur and De Mori, 2011) are two fundamental tasks in spoken language understanding (SLU) (Young et al., 2013) which is a core component in the dialog systems. In recent years, a bunch of joint models (Liu and Lane, 2016; Goo et al., 2018; Li et al., 2018; Liu et al., 2019a; E et al., 2019; Qin et al., 2019; Zhang et al., 2019; Qin et al., 2021b) have been proposed to tackle single intent detection and slot filling at once via modeling their correlations.

In real-world scenarios, a single utterance usually expresses multiple intents. To handle this, multi-intent SLU (Kim et al., 2017) is explored and Gangadharaiyah and Narayanaswamy (2019) first

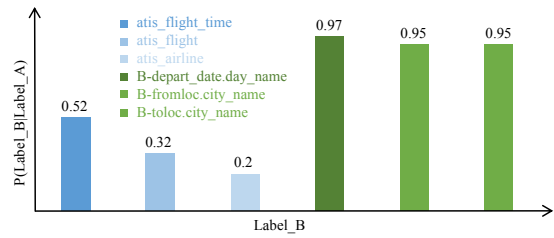


Figure 1: Illustration of top-3 high-probability occurring intent (in blue) and slot (in green) labels when B-depart\_date.date\_relative (Label\_A) occurs in the training samples of MixATIS dataset.

propose to jointly model the multiple intent detection and slot filling in a multi-task framework. Qin et al. (2020) and Qin et al. (2021c) further utilize graph attention networks (GATs) (Velickovic et al., 2018) which model the interactions between the embeddings of predicted intent labels and the semantic hidden states of slot filling task to leverage the dual-task correlations in an explicit way. And significantly improvements have been achieved.

However, we argue that previous works are essentially limited by ignoring the rich topological structures and relations in the joint label space of the two tasks because they treat the embeddings of intent labels and slot labels as individual parameter vectors to be learned. Based on our observation, there are two kinds of potential topological structures in the joint label space. (1) The global statistical dependencies among the labels based on their co-occurrence patterns, which we discover are widely-existing phenomenons. Fig. 1 shows an example of label co-occurrence. (2) The hierarchies in the slot labels. Although there is no officially predefined slot label hierarchy in the datasets, we discover and define two kinds of hierarchies. An example is shown in Fig. 2. Firstly, it is intuitive that there is an intrinsic dependency between a B-slot label and its I-slot label: in the slot sequence of an utterance, an I-slot label must occur after its B-slot label, and an I-slot cannot occur solely.

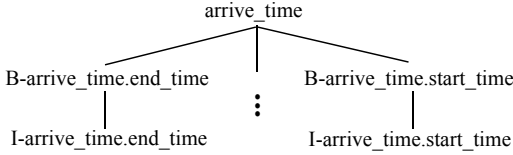


Figure 2: Illustration of the hierarchy between the pseudo label `arrive_time` and B- slot labels, and the hierarchy between the B- slot label and its I- label.

Therefore, in the label space, there should be a hierarchy between a B- slot and its I- slot, while existing methods regard all slot labels as independent ones. Secondly, we discover that some B- slot labels share the same prefix, which indicates their shared semantics. Therefore, the prefix can be regarded as a pseudo slot label connecting these slot labels. We believe the above statistical dependencies and hierarchies can help to capture the inner- and inter-task label correlations which benefit the joint task reasoning. Thus in this paper, we focus on exploiting the label topologies and relations for tackling the joint task.

Besides, previous models decode the two tasks' hidden states independently without leveraging the dual-task correlations. This causes the misalignment of the two tasks' correct predictions. As a result, the performance (Overall Accuracy) on sentence-level semantic frame parsing is much worse than the two tasks. Therefore, we argue that the label embeddings conveying the dual-task correlative information should be leveraged in the decoders to guide the decoding process.

To overcome the above challenges, in this paper, we first construct a heterogeneous label graph (HLG) including both the global statistical dependencies and slot label hierarchies, based on which we define a bunch of edge types to represent the topological structures and rich relations among the labels. Then we propose a novel model termed **Recurrent heterogeneous Label matching Network** (ReLa-Net) to capture the beneficial label correlative information from HLG and sufficient leverage them for tackling the joint task. To capture the label correlative information from HLG, we design a Heterogeneous Label Graph Transformations (HLGT) module, which conducts relation-specific information aggregation among the label nodes. We design a recurrent dual-task interacting module to leverage label correlations for semantics-label interactions. At each step, it takes both tasks' semantic hidden states and label knowledge generated at the previous step as input. Then sequence-

reasoning BiLSTM (Hochreiter and Schmidhuber, 1997) and GATs (Velickovic et al., 2018) are utilized for interactions. As for decoding, we design a novel label-aware inter-dependent decoding mechanism that takes both the hidden states and label embeddings as input and measures their correlation scores in the joint label embedding space. By this means, the joint label embedding space serves as a bridge to connect the two tasks' decoding processes which then can be guided by the dual-task inter-dependencies conveyed in the learned label embeddings. We evaluate our ReLa-Net on benchmark datasets and the results show that ReLa-Net achieves new state-of-the-art performance. Further analysis proves that our method can capture non-trivial correlations among the two tasks' labels and effectively leverage them to tackle the joint task.

## 2 Problem Definition

Given a utterance  $\mathcal{U}$ , the task of joint multiple intent detection and slot filling aims to output a intent label set  $O^I = \{o_1^I, \dots, o_m^I\}$  and a slot label sequence  $O^S = \{o_1^S, \dots, o_n^S\}$ , where  $n$  is the length of  $\mathcal{U}$  and  $m$  is the number of intents expressed in  $\mathcal{U}$ .

## 3 Heterogeneous Label Graph

Mathematically, the HLG can be denoted as  $\mathcal{G} = (\mathcal{V}, \mathcal{E}, \mathcal{A}, \mathcal{R})$ , where  $\mathcal{V}$  is the set of nodes,  $\mathcal{E}$  is the set of edges,  $\mathcal{A}$  is the set of node types and  $\mathcal{R}$  is the set of relations or edge types. As shown in Fig. 3, there are three types of nodes: intent nodes, slot nodes, and pseudo nodes, which correspond to the intent labels, slot labels, and pseudo slot labels.

In HLG, there are two kinds of topologies, which correspond to statistical and hierarchical dependencies, respectively. To represent and capture these dependencies, we define 12 relations on HLG:  $r_1 \sim r_8$  for statistical dependencies and  $r_9 \sim r_{12}$  for hierarchical dependencies, whose definitions are shown in Table 1. And  $|\mathcal{V}| = N^I + N^S + N^P$ , in which  $N^I$ ,  $N^S$  and  $N^P$  denote the numbers of intent nodes, slot nodes and pseudo nodes.

$r_1 \sim r_8$  are based on the conditional probability between two labels, and two thresholds  $(\lambda_1, \lambda_2)$  are used to determine whether there is statistical dependency or strong statistical dependency from node  $i$  to node  $j$  regarding  $P(j|i)$ . A high value of  $P(j|i)$  denotes that when label  $i$  occurs, there always exists label  $j$  in the sample. Namely, label  $j$  can be potentially deduced when label  $i$  is predicted. In this case, an edge is established from node  $i$  to

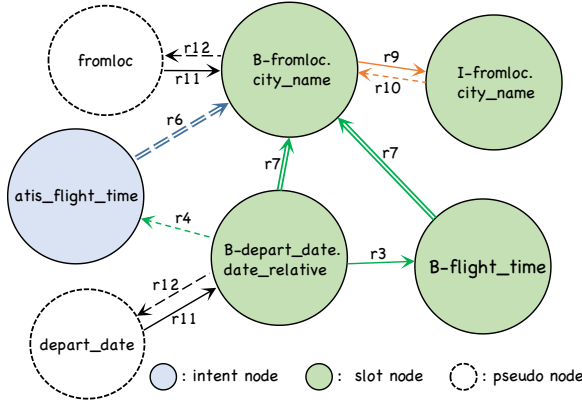


Figure 3: Illustration of a snippet from the whole HLG.

$\phi(e_{ij})$	$\tau(i)$	$\tau(j)$	$P(j i)$
$r_1: i2i\_stat\_dep$	intent	intent	$\lambda_1 \leq p < \lambda_2$
$r_2: i2s\_stat\_dep$	intent	slot-B	$\lambda_1 \leq p < \lambda_2$
$r_3: s2s\_stat\_dep$	slot-B	slot-B	$\lambda_1 \leq p < \lambda_2$
$r_4: s2i\_stat\_dep$	slot-B	intent	$\lambda_1 \leq p < \lambda_2$
$r_5: i2i\_stat\_strong\_dep$	intent	intent	$p \geq \lambda_2$
$r_6: i2s\_stat\_strong\_dep$	intent	slot-B	$p \geq \lambda_2$
$r_7: s2s\_stat\_strong\_dep$	slot-B	slot-B	$p \geq \lambda_2$
$r_8: s2i\_stat\_strong\_dep$	slot-B	intent	$p \geq \lambda_2$
$r_9: b2i\_hierarchy$	slot-B	slot-I	\
$r_{10}: i2b\_hierarchy$	slot-I	slot-B	\
$r_{11}: parent2child\_hierarchy$	pseudo	slot-B	\
$r_{12}: child2parent\_hierarchy$	slot-B	pseudo	\

Table 1: Illustration of the definition of the 12 relations in HLG.  $\phi(e_{ij})$  denotes the relation of edge  $e_{ij}$  (from  $i$  to  $j$ ).  $\tau(i)$  denotes what kinds of label the node  $i$  corresponds to.  $P(j|i)$  denotes the conditional probability of a sample having a label  $j$  when it has a label  $i$ .

node  $j$  with the corresponding relation. Note that in each sample, most slot labels are  $\circ$  which denotes the word has no meaningful slot. Considering the slot label  $\circ$  cannot provide valuable clues, although it has high conditional probabilities (always 1.0) with other labels. Therefore, the slot node  $\circ$  is set as an isolated node in HLG.

$r_1 \sim r_8$  are based on the hierarchies we discovered in slot labels. A B- slot node can connect and interact with many nodes, including intent nodes, other B- slot nodes, its parent pseudo node, and its I- slot node. Differently, an I- slot node only connects with its B- slot nodes because there is a natural affiliation relation between a pair of B- and I- slot labels: an I- slot label can only appear after its B-slot label. As for the pseudo labels we defined, there is a parent-child relationship between the parent pseudo labels and their child B- slot labels. In HLG, a pseudo label works like an information station, which allows its children (B- slot nodes) to share their semantics and features.

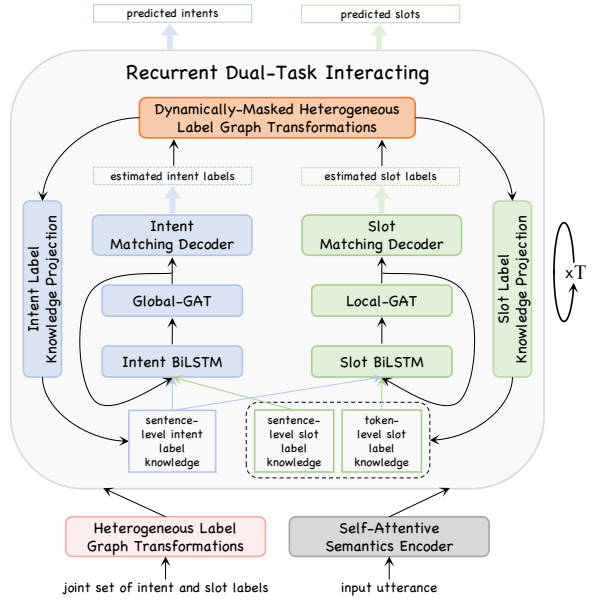


Figure 4: The network architecture of our ReLa-Net.

## 4 ReLa-Net

**Overview.** The architecture of our ReLa-Net is shown in Fig. 4. Firstly, the initial label embeddings containing beneficial label correlations are generated by the proposed Heterogeneous Label Graph Transformations (HLGT) module, and the initial semantic hidden states are generated by the Self-Attentive Semantics Encoder. Then we allow the two tasks to interact recurrently. At each time step, for each task, the semantic hidden states and the label knowledge of both tasks are fused, and their correlations are learned in a BiLSTM and then a GAT. Then the designed Label-Aware Inter-Dependent Decoding mechanism produces the estimated labels via measuring the correlations between the hidden state and the label embeddings. The obtained labels are fed to the designed Dynamically-Masked Heterogeneous Label Graph Transformations (DM-HLGT) module, which dynamically derives the sample-specific label knowledge via operating on a DM subgraph of HLG. Then the obtained label knowledge is used at the next time step. Finally, after  $T$  step, the last produced labels are taken as the final predictions.

Next, we introduce the details of each module.

### 4.1 HLGT

To capture the correlations among the intent and slot labels, inspired by (Schlichtkrull et al., 2018; Xing and Tsang, 2022a), we conduct relation-specific graph transformations to achieve informa-

tion aggregation on HLG:

$$e_i^l = \text{ReLU}(W_1 e_i^{l-1} + \sum_{r \in \mathcal{R}} \sum_{j \in \mathcal{N}_i^r} \frac{1}{|\mathcal{N}_i^r|} W_1^r e_j^{l-1}) \quad (1)$$

where  $l$  denotes the layer number;  $\mathcal{N}_i^r$  denotes the set of node  $i$ 's neighbors which are connected to it with  $r$ -type edges;  $W_1$  is self weight matrix and  $W_1^r$  is relation-specific weight matrix. The initial node representations are obtained from an initialized matrix which is trained with the model.

After  $L$  layers, the initial intent label embedding matrix  $E^I$  and slot label embedding matrix  $E^S$  are obtained. Although  $E^I$  and  $E^S$  contain beneficial correlative information, the HLG is globally built on the whole train set. Therefore, they are not flexible enough for every sample, whose labels may form a local subgraph on HLG. And we believe capturing the sample-specific label correlations can further enhance the reasoning by discovering potential neighbor labels. To this end, we propose the Dynamically-Masked HLG, which will be introduced in Sec. 4.3.4.

## 4.2 Self-Attentive Semantics Encoder

Following previous works, we adopt the self-attentive encoder (Qin et al., 2020, 2021c) to generate the initial semantic hidden states. It includes a BiLSTM (Hochreiter and Schmidhuber, 1997) and a self-attention mechanism (Vaswani et al., 2017). The input utterance's word embeddings are fed to the BiLSTM and self-attention separately. Then the two streams of word representations are concatenated as the output semantic hidden states.

## 4.3 Recurrent Dual-Task Interacting

### 4.3.1 Semantics-Label Interaction

BiLSTM has been proven to be capable of sequence reasoning (Vaswani et al., 2016; Katiyar and Cardie, 2016; Zheng et al., 2017). In this paper, we utilize two BiLSTMs for intent and slot to achieve the fusion and interactions among the semantics and label knowledge of both tasks. Specifically, the two BiLSTMs can be formulated as:

$$\begin{aligned} \hat{h}_t^{I,i} &= \text{BiLSTM}_I(h_t^{I,i} \| K_t^I \| K_t^S, \hat{h}_t^{I,i-1}, \hat{h}_t^{I,i+1}) \\ \hat{h}_t^{S,i} &= \text{BiLSTM}_S(h_t^{S,i} \| K_t^I \| K_t^S, \hat{h}_t^{S,i-1}, \hat{h}_t^{S,i+1}) \end{aligned} \quad (2)$$

where  $\|$  denotes concatenation operation.

For Intent BiLSTM ( $\text{BiLSTM}_I$ ), the input is the concatenation of intent semantic hidden states  $h_t^{I,i}$ , sentence-level intent label knowledge  $K_t^I$  and the sentence-level slot label knowledge  $K_t^S$ , where  $t$

denotes the step number of recurrent dual-task interacting. Here we use sentence-level label knowledge because multiple intent detection is on sentence-level. For Slot BiLSTM ( $\text{BiLSTM}_S$ ), the input is the concatenation of slot semantic hidden states  $h_t^{S,i}$ , sentence-level intent label knowledge  $K_t^I$  and the token-level slot label knowledge  $K_t^{S,i}$ . Here we use token-level slot label knowledge because slot filling is a token-level task. And we use sentence-level intent label knowledge here because it can provide indicative clues of potential slot labels regarding the captured inter-task dependencies among intent and slot labels.

At the first step, there is no available label knowledge, so the inputs of the two BiLSTMs are the initial hidden states generated in Sec. 4.2. How to obtain  $K_t^I, K_t^S, K_t^{S,i}$  is depicted in Sec. 4.3.5.

### 4.3.2 Graph Attention Networks

**Global-GAT** Since multiple intent detection is a sentence-level task, we believe it is beneficial to further capture the global dependencies among the words. We first construct a fully-connected graph on the input utterance. There are  $n$  nodes in this graph and each one corresponds to a word. And we adopt the GAT (Velickovic et al., 2018) for information aggregation. The initial representation of node  $i$  is  $\hat{h}_t^{I,i}$  generated by  $\text{BiLSTM}_I$ . After  $L$  layers, we obtain  $\tilde{H}_t^I = \{\tilde{h}_t^{I,i}\}_{i=1}^N$ .

**Local-GAT** Since slot filling is on token-level, we adopt a Local-GAT to capture the token-level local dependencies. The Local-GAT works on a locally-connected graph where node  $i$  is connected to nodes  $\{i-w, \dots, i+w\}$ , where sliding window size  $w$  is a hyper-parameter. The initial representation of node  $i$  is  $\hat{h}_t^{S,i}$  generated by  $\text{BiLSTM}_S$ . After  $L$  layers, we obtain  $\tilde{H}_t^S = \{\tilde{h}_t^{S,i}\}_{i=1}^N$ . And we adopt the GAT (Velickovic et al., 2018) for information aggregation.

### 4.3.3 Label-Aware Inter-Dependent Decoding

In this work, we design a novel label-aware inter-dependent decoding mechanism (shown in Fig. 5) to leverage the dual-task correlative information conveyed in the learned label embeddings to guide the decoding process. Concretely, the hidden state is first projected into the joint label embedding space, and then the dot products are conducted between it and all label embeddings of a specific task to obtain the correlation score vector. The larger

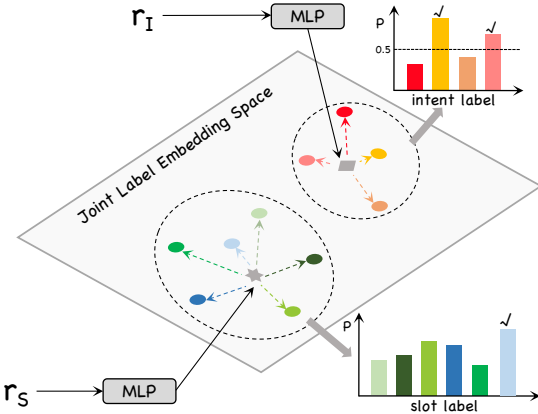


Figure 5: Illustration of our proposed label-aware co-decoding mechanism. Blue/green circles denote slot labels and red/yellow circles denote intent labels. The dash arrow denotes the distance between the hidden state projection and the label. The shorter the distance, the greater the probability that the label is correct. ✓ denotes that the label is selected as the prediction.

correlation score indicates the shorter distance between the hidden state’s projection and the label embedding. Thus the hidden state more likely belongs to the corresponding class. In this way, the joint label embedding space serves as a bridge that connects the decoding processes of the two tasks, and the beneficial correlative information conveyed in the learned label embeddings can guide the inter-dependent decoding for the two tasks. Next, we introduce the intent and slot decoders in details.

**Intent Decoder** Following previous works, we conduct token-level multi-label classification. Firstly, the intent hidden state  $\tilde{h}_t^{I,i}$  is projected into the joint label embedding space via an MLP. Then the correlation score vector  $C_t^{I,i}$  is calculated via dot products between it and all intent label embeddings. This process can be formulated as:

$$C_t^{I,i} = (W_I(\text{LeakyReLU}(W_h^I \tilde{h}_t^{I,i} + b_h)) + b_I) \hat{E}_t^I \quad (3)$$

where  $C_t^{I,i}$  is a  $N^I$ -dimensional vector;  $\hat{E}_t^I$  is the sample-specific intent label embedding matrix at step  $t$ ;  $W_*$  and  $b_*$  are model parameters.

Then  $C_t^{I,i}$  is fed to the sigmoid function to obtain the token-level intent probability vector. And a threshold (0.5) is used to select the intents. Finally, we obtain the predicted sentence-level intents by voting for all tokens’ intents (Qin et al., 2021c).

**Slot Decoder** Following (Qin et al., 2021c), we conduct parallel decoding. Similar to Eq. 3, the slot correlation score vector  $C_t^{S,i}$  is obtained by:

$$C_t^{S,i} = (W_S(\text{LeakyReLU}(W_h^S \tilde{h}_t^{S,i} + b_S)) + b_S) \hat{E}_t^S \quad (4)$$

where  $C_t^{S,i}$  is a  $N^S$ -dimensional vector;  $\hat{E}_t^S$  is the sample-specific slot label embedding matrix at step  $t$ ;  $W_*$  and  $b_*$  are model parameters.

Then  $C_t^{I,i}$  is fed to the softmax function to obtain the slot probability distribution. Finally, the argmax function is used to select the predicted slot.

#### 4.3.4 DM-HLGT

After decoding, we obtain the predicted intents and slots at step  $t$ . To capture the sample-specific label correlations, which we believe further benefit the reasoning in the next step, we first construct a DM subgraph of HLG for each sample. The process is simple: the nodes of predicted intent labels and slot labels and their first-order neighbors are reserved, while other nodes on HLG are masked out. Then relation-specific graph transformations are conducted on this graph to achieve information aggregation, whose formulation is similar to Eq. 1. At the first step, the  $\hat{E}_0^I$  and  $\hat{E}_0^S$  are  $E^I$  and  $E^S$ .

#### 4.3.5 Label Knowledge Projection

To provide label knowledge for next time step, the predicted labels should be projected into vectors. In Sec. 4.3.1, we use three kinds of label knowledge:  $K_t^I, K_t^S, K_t^{S,i}$ .  $K_t^I$  and  $K_t^S$  are sentence-level intent and slot label knowledge, respectively.  $K_t^I$  is the sum of label embeddings of the predicted intents and  $K_t^S$  is the sum of label embeddings of the predicted slots while the  $\textcircled{O}$  slot is excluded.  $K_t^{S,i}$  is token-level slot label knowledge, which is the label embedding of the predicted slot of token  $t$ .

### 4.4 Optimization

Following previous works, the standard loss function for intent task ( $\mathcal{L}_I$ ) and slot task ( $\mathcal{L}_S$ ) are:

$$\begin{aligned} l(\hat{y}, y) &= \hat{y} \log(y) + (1 - \hat{y}) \log(1 - y) \\ \mathcal{L}_I &= \sum_{t=1}^T \sum_{i=1}^n \sum_{j=1}^{N^I} l(\hat{y}_i^I[j], y_i^{I,t}[j]) \\ \mathcal{L}_S &= \sum_{t=1}^T \sum_{i=1}^n \sum_{j=1}^{N^S} \hat{y}_i^S[j] \log(y_i^{[S,t]}[j]) \end{aligned} \quad (5)$$

Besides, we design a constraint loss ( $\mathcal{L}_{cst}$ ) to push ReLa-Net to generate better label distributions at step  $t$  than step  $t - 1$ :

$$\mathcal{L}_{cons}^I = \sum_{t=2}^T \sum_{i=1}^n \sum_{j=1}^{N^I} \hat{y}_i^I[j] \max(0, y_i^{[I,t-1]}[j] - y_i^{[I,t]}[j]) \quad (6)$$

And  $\mathcal{L}_{cst}^S$  can be derived similarly.

Then the final training objective is:

$$\mathcal{L} = \gamma_I (\mathcal{L}_I + \beta_I \mathcal{L}_{cst}^I) + \gamma_S (\mathcal{L}_S + \beta_S \mathcal{L}_{cst}^S) \quad (7)$$

where  $\gamma_I = 0.1$  and  $\gamma_S = 0.9$  balance the two tasks;  $\beta_I = 0.01$  and  $\beta_S = 1.0$  balance the standard loss and constraint loss for the two tasks.

## 5 Experiments

### 5.1 Settings

**Datasets.** Following previous works, we conduct experiments on two benchmarks: MixATIS and MixSNIPS (Hemphill et al., 1990; Coucke et al., 2018; Qin et al., 2020). In MixATIS, the split of train/dev/test set is 13162/756/828 (utterances). In MixSNIPS, the split of train/dev/test set is 39776/2198/2199 (utterances).

**Evaluation Metrics.** Following previous works, we evaluate multiple intent detection using accuracy (Acc), slot filling using F1 score, and sentence-level semantic frame parsing using overall Acc. Overall Acc denotes the ratio of utterances for which both intents and slots are predicted correctly.

**Implementation Details.** Following previous works, the word and label embeddings are randomly initialized and trained with the model. Due to limited space, the experiments using pre-trained language model is presented in the Appendix. The dimension of the word/label embedding is 128 on MixATIS and 256 on MixSNIPS. For HLG,  $\lambda_1 = 0.4$  and  $\lambda_2 = 0.9$ . The hidden dim is 200. The max layer number of all GNNs is 2. Max time step  $T$  is 2. We adopt Adam (Kingma and Ba, 2015) optimizer to train our model using the default setting. For all experiments, we select the best model on the dev set and report its results on the test set. Our source code will be released.

### 5.2 Main Results

We compare our model with: (1) Attention BiRNN (Liu and Lane, 2016); (2) Slot-Gated (Goo et al., 2018); (3) Bi-Model (Wang et al., 2018); (4) SF-ID Network (E et al., 2019); (5) Stack-Propagation (Qin et al., 2019); (6) Joint Multiple ID-SF (Tur and De Mori, 2011); (7) AGIF (Qin et al., 2020); (8) GL-GIN (Qin et al., 2021c). Table 2 lists the results on the test sets. We can observe that:

1. Our Rela-Net consistently outperforms all baselines by large margins on all datasets and tasks. Specifically, compared with Gl-GIN, the previous best model, ReLa-Net achieves an absolute improvement of 9.2% in terms of Overall Acc on

Models	MixATIS			MixSNIPS		
	Overall (Acc)	Slot (F1)	Intent (Acc)	Overall (Acc)	Slot (F1)	Intent (Acc)
Attention BiRNN	39.1	86.4	74.6	59.5	89.4	95.4
Slot-Gated	35.5	87.7	63.9	55.4	87.9	94.6
Bi-Model	34.4	83.9	70.3	63.4	90.7	95.6
SF-ID	34.9	87.4	66.2	59.9	90.6	95.0
Stack-Propagation	40.1	87.8	72.1	72.9	94.2	96.0
Joint Multiple ID-SF	36.1	84.6	73.4	62.9	90.6	95.1
AGIF	40.8	86.7	74.4	74.2	94.2	95.1
GL-GIN	43.0	88.2	76.3	73.7	94.0	95.7
ReLa-Net (ours)	<b>52.2</b>	<b>90.1</b>	<b>78.5</b>	<b>76.1</b>	<b>94.7</b>	<b>97.6</b>

Table 2: Main results. ReLa-Net obtains statistically significant improvements over baselines with  $p < 0.01$ .

- MixATIS, a relative improvement of over 20%.  
2. ReLa-Net gains larger improvements on the intent task than slot task. The reason is that ReLa-Net is the first model to allow the two tasks to interact with each other, while previous models only leverage the predicted intents to guide slot filling.  
3. Generally, the results on overall Acc are obviously worse than slot F1 and intent Acc, indicating that it is hard to align the correct prediction of intents and slots. Compared with baselines, our ReLa-Net achieves especially significant improvements on overall Acc and effectively reduces the performance gap between overall Acc and slot F1/intent Acc. This can be attributed to the fact that our model can capture the sufficient and beneficial label correlations from HLG, and the designed label-aware inter-dependent decoding mechanism can leverage the label correlations to guide decoding, making the two tasks’ decoding processes correlative. As a result, the correct predictions of the two tasks are better aligned.  
4. ReLa-Net gains more significant improvements on MixATIS dataset than MixSNIPS. The reason is that MixATIS dataset includes much more labels than MixSNIPS: MixATIS includes 17 intent labels and 117 slot labels, while MixSNIPS only include 7 intent labels and 72 slot labels. More labels in MixATIS dataset cause it is much harder for correct predictions, which can be proved by the lower Overall Acc scores of all models on MixATIS than MixSNIPS. However, the core strength of our model is leveraging the label topologies and relations. Therefore, more labels in MixATIS dataset result in larger improvements.

### 5.3 Ablation Study

We conduct two groups of ablation experiments on HLG and ReLa-Net to verify the necessities of

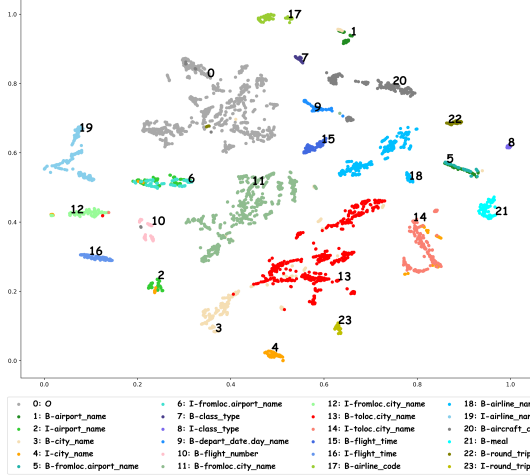


Figure 6: Visualization of ReLa-Net’s slot clusters.

their components. Table 3 shows the results.

**HLG. w/o *stat\_dep*** denotes the statistical dependencies are removed, which means there are no edges between intent and slot label nodes on HLG. We can observe sharp drops in the performances of two tasks and the semantic frame parsing. This proves that statistical dependencies can effectively capture the beneficial inter-task dependencies. **w/o *hierarchy*** denotes the slot hierarchies are removed. We can find although Intent Acc is not seriously affected, the Slot F1 and Overall Acc are both significantly reduced. This proves that slot hierarchies can effectively bring improvements via capturing the beneficial structural dependencies among slot labels. **w/o *relation*** denotes HLG collapses into a homogeneous graph without specific relations. Its poor performances prove that the defined rich relations on HLG are crucial for capturing the label correlations, which play key roles in dual-task reasoning and label-aware inter-dependent decoding.

**ReLa-Net. w/o *matching*** denotes the designed matching decoders in ReLa-Net are replaced with the linear decoders used in previous models. Its worse results prove that our designed matching de-

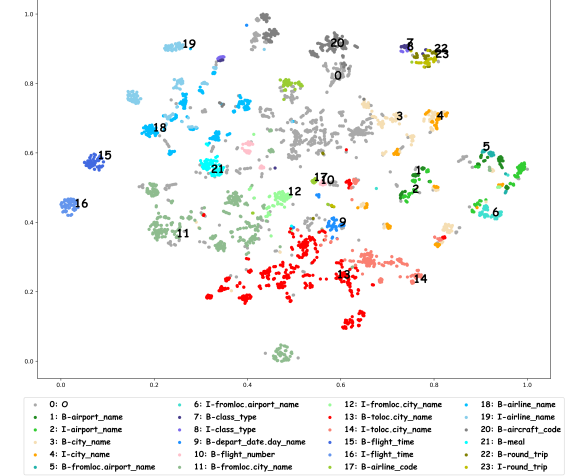


Figure 7: Visualization of GL-GIN’s slot clusters.

coders can effectively improve the decoding quality via leveraging the beneficial label correlations captured from HLG. **w/o *GATs*** denotes the Global-GAT and Local-GAT are removed. Its worse results prove that the sentence-level global dependencies and the token-level local dependencies are important for the intent task and slot task, respectively. However, even if its semantics and semantics-label interactions are only modeled via LSTM, it still outperforms all baselines. This can be attributed to the fact that ReLa-Net can learn beneficial label correlations from HLG and sufficiently leverage them for decoding. **w/o *DM-HLGT*** denotes the DM-HLGT is removed. And its results verify that DM-HLGT can effectively enhance the performance via capturing the sample-specific label correlations and discovering potential neighbor labels.

#### 5.4 Visualization of Hidden State Clusters

To better understand the promising results of ReLa-Net, we perform TSNE (van der Maaten and Hinton, 2008) visualization on the final hidden states of the utterances words in the test set of MixATIS. It is hard to visualize intent states because a single hidden state usually corresponds to multiple intents. Therefore, we visualize the final slot hidden state of each word in the utterances. Since there are more than 100 slot labels, to simply the visualization, we rank the slot labels regarding their frequencies in the test set, and we show the results of the top-24 labels. Besides, most slot labels in the test set are  $\text{O}$ , and we randomly pick 500 ones. The slot clusters visualization of our ReLa-Net is shown in Fig. 6.

From Fig. 6, we can observe that the boundaries of the clusters are clear, and the data points

Variants	MixATIS		
	Overall (Acc)	Slot (F1)	Intent (Acc)
ReLa-Net	<b>52.2</b>	<b>90.1</b>	<b>78.5</b>
w/o <i>stat_dep</i>	45.3( $\downarrow$ 6.9)	87.5( $\downarrow$ 2.6)	76.9( $\downarrow$ 1.6)
w/o <i>hierarchy</i>	48.4( $\downarrow$ 3.8)	87.9( $\downarrow$ 2.2)	78.1( $\downarrow$ 0.4)
w/o <i>relation</i>	45.1( $\downarrow$ 7.1)	88.2( $\downarrow$ 1.9)	75.4( $\downarrow$ 3.1)
w/o <i>matching</i>	45.2( $\downarrow$ 7.0)	88.1( $\downarrow$ 2.0)	77.4( $\downarrow$ 1.1)
w/o <i>GATs</i>	47.6( $\downarrow$ 4.6)	88.3( $\downarrow$ 1.8)	77.2( $\downarrow$ 1.3)
w/o <i>DM-HLGT</i>	50.2( $\downarrow$ 2.0)	89.2( $\downarrow$ 0.9)	78.0( $\downarrow$ 0.5)

Table 3: Results of ablation experiments.

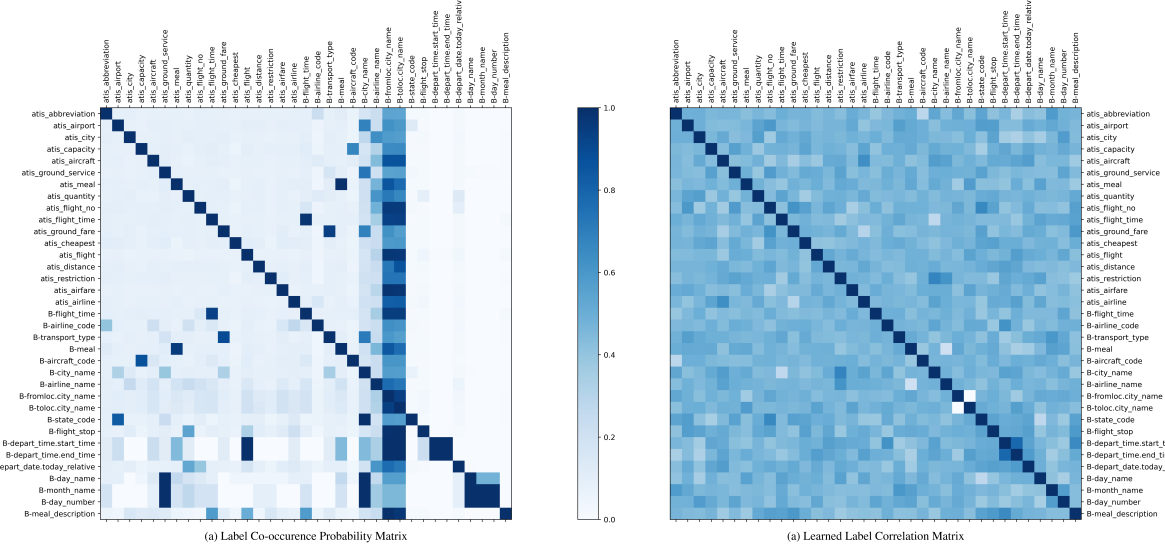


Figure 8: Visualization of label co-occurrence matrix and learned label correlation matrix.

in the same cluster are tightly closed to each other. And we can find that the B- slot clusters and their corresponding I- slot clusters are clearly separated. Besides, there is nearly no incorrect I- slot data point. The high accuracy of I- slot labels prove that our ReLa-Net effectively resolves the uncoordinated slot problem (e.g., B-singer followed by I-song). This is attributed to the beneficial slot hierarchies we discovered and leveraged.

For comparison, we visualize GL-GIN’s slot clusters in the same way, as shown in Fig. 7. We can observe that GL-GIN’s slot clusters boundaries are not clear. Some data points of ‘O’ slot are close to other clusters. And some B- clusters and their I-clusters even significantly overlap each other.

Above observations prove that our method can learn better hidden states via effectively capturing and leveraging the label correlations.

### 5.5 Visualization of Label Correlations

To further look into the label correlations, we visualize the label co-occurrence probability matrix constructed from MixATIS training set and the correlation matrix of ReLa-Net’s learned label embeddings, as shown in Fig. 8 (a) and (b). Label correlations of two labels are measured by the cosine similarity of their embeddings. For simplification, we visualize all intent labels (17 ones) and some slot labels (18 ones). From Fig 8 (a), we can observe that there exist many distinct co-occurrence patterns among the labels of the two tasks. The core of this work is capturing and leveraging the beneficial label correlations, and promising improvements have

been observed from the experiment results, while previous works neglect this point. From Fig. 8 (b), we can find that our ReLa-Net learns non-trivial label embeddings. From the patterns of label correlations in Fig. 8 (b), we can hardly observe the label co-occurrence patterns in Fig. 8 (a). This proves that ReLa-Net can comprehensively leverage the label co-occurrences to learn robust and effective label embeddings, rather than just mechanically memorize them.

## 6 Related Work

To capture and leverage the dual-task correlations, a group of models (Zhang and Wang, 2016; Hakkani-Tür et al., 2016; Goo et al., 2018; Li et al., 2018; E et al., 2019; Liu et al., 2019a; Qin et al., 2019; Zhang et al., 2019; Wu et al., 2020; Qin et al., 2021b; Ni et al., 2021) have been proposed for joint intent detection and slot filling. However, they only consider the single-intent scenario. Unlike them, we tackle the joint task of multiple intent detection and slot filling, which is more challenging and practical in the real-world scenario.

Recently, multi-intent SLU has received increasing attention since it can handle complex utterances expressing multiple intents. Kim et al. (2017) propose a two-stage model to tackle the multiple intent detection task. And Gangadharaiyah and Narayanaswamy (2019) propose the first joint model that employs a multi-task framework including a slot-gate mechanism to tackle the joint task of multiple intent detection and slot filling. With the wide utilization of graph neural networks

(GNNs) in various NLP tasks (Lin et al., 2019; Fang et al., 2020; Qin et al., 2021a; Xing and Tsang, 2022b,c,d,e), state-of-the-art multi-intent SLU systems also leverage GNNs to model the cross-task interactions. Qin et al. (2020) utilize GATs to introduce the fine-grained information of the predicted multiple intents into slot filling in an adaptive way. Further, Qin et al. (2021c) propose a GAT-based model in which slot filling is conducted in a non-autoregressive manner.

Previous models ignore the correlations among the two tasks’ labels, treating their embeddings as separated parameters to be learned. Our method is significantly different from previous ones. This is the first work to discover, capture and leverage the topologies and relations among the labels for joint multiple intent detection and slot filling.

## 7 Conclusion

In this work, we improve joint multiple intent detection and slot filling from a new perspective: exploiting label typologies and relations. Specifically, we first design a heterogeneous label graph to represent the statistical dependencies and hierarchies in rich relations. Then we propose a recurrent heterogeneous label matching network to end-to-end capture and leverage the beneficial label correlations. Experiments demonstrate that our method significantly outperforms previous models, achieving new state-of-the-art. Further studies verify the advantages of our methods and show that our model can generate better hidden states and learns non-trivial label embeddings. In the future, we will apply our method in other multi-task scenarios.

## Limitations

The core of this work is proving the power of the learned label embeddings obtained by exploiting label topologies and relations. Therefore, to better demonstrate that the significant improvements come from the learned label embeddings, we do not focus on enhancing the interactions between the label knowledge and semantics. We adopt BiLSTM, a relatively basic module, to model the interactions between the prediction information and semantics. However, there is no doubt that BiLSTM is not the optimal module for these label-semantics interactions, and in practice, many modules can be applied to achieve this better. For instance, GL-GIN adopts not only BiLSTM but the proposed global-locally graph interaction layers working on the designed

label-semantic graph to model the label-semantics interactions. Therefore, although our ReLa-Net significantly outperforms state-of-the-art models, intuitively, its performance is limited by the simple module for modeling the label-semantics interactions. In our future work, we will design more advanced modules for semantics-label interactions.

## Acknowledgements

This work was supported by Australian Research Council Grant DP200101328. Bowen Xing and Ivor W. Tsang was also supported by A\*STAR Centre for Frontier AI Research.

## References

- Alice Coucke, Alaa Saade, Adrien Ball, Théodore Bluche, Alexandre Caulier, David Leroy, Clément Doumouro, Thibault Gisselbrecht, Francesco Caltagirone, Thibaut Lavril, Maël Primet, and Joseph Dureau. 2018. Snips voice platform: an embedded spoken language understanding system for private-by-design voice interfaces.
- Haihong E, Peiqing Niu, Zhongfu Chen, and Meina Song. 2019. A novel bi-directional interrelated model for joint intent detection and slot filling. In *Proceedings of the 57th Annual Meeting of the Association for Computational Linguistics*, pages 5467–5471, Florence, Italy. Association for Computational Linguistics.
- Yuwei Fang, Siqi Sun, Zhe Gan, Rohit Pillai, Shuhang Wang, and Jingjing Liu. 2020. Hierarchical graph network for multi-hop question answering. In *Proceedings of the 2020 Conference on Empirical Methods in Natural Language Processing (EMNLP)*, pages 8823–8838, Online. Association for Computational Linguistics.
- Rashmi Gangadharai and Balakrishnan Narayanaswamy. 2019. Joint multiple intent detection and slot labeling for goal-oriented dialog. In *Proceedings of the 2019 Conference of the North American Chapter of the Association for Computational Linguistics: Human Language Technologies, Volume 1 (Long and Short Papers)*, pages 564–569, Minneapolis, Minnesota. Association for Computational Linguistics.
- Chih-Wen Goo, Guang Gao, Yun-Kai Hsu, Chih-Li Huo, Tsung-Chieh Chen, Keng-Wei Hsu, and Yun-Nung Chen. 2018. Slot-gated modeling for joint slot filling and intent prediction. In *Proceedings of the 2018 Conference of the North American Chapter of the Association for Computational Linguistics: Human Language Technologies, Volume 2 (Short Papers)*, pages 753–757, New Orleans, Louisiana. Association for Computational Linguistics.

- Dilek Hakkani-Tür, Gokhan Tur, Asli Celikyilmaz, Yun-Nung Chen, Jianfeng Gao, Li Deng, and Ye-Yi Wang. 2016. *Multi-domain joint semantic frame parsing using bi-directional rnn-lstm*. In *Interspeech 2016*, pages 715–719.
- Charles T. Hemphill, John J. Godfrey, and George R. Doddington. 1990. *The ATIS spoken language systems pilot corpus*. In *Speech and Natural Language: Proceedings of a Workshop Held at Hidden Valley, Pennsylvania, June 24-27, 1990*.
- Sepp Hochreiter and Jürgen Schmidhuber. 1997. *Long short-term memory*. *Neural Computation*, 9(8):1735–1780.
- Arzoo Katiyar and Claire Cardie. 2016. *Investigating LSTMs for joint extraction of opinion entities and relations*. In *Proceedings of the 54th Annual Meeting of the Association for Computational Linguistics (Volume 1: Long Papers)*, pages 919–929, Berlin, Germany. Association for Computational Linguistics.
- Byeongchang Kim, Seonghan Ryu, and Gary Geunbae Lee. 2017. *Two-stage multi-intent detection for spoken language understanding*. *Multimedia Tools and Applications*, 76(9):11377–11390.
- Diederik P. Kingma and Jimmy Ba. 2015. *Adam: A method for stochastic optimization*. In *3rd International Conference on Learning Representations, ICLR 2015, San Diego, CA, USA, May 7-9, 2015, Conference Track Proceedings*.
- Changliang Li, Liang Li, and Ji Qi. 2018. *A self-attentive model with gate mechanism for spoken language understanding*. In *Proceedings of the 2018 Conference on Empirical Methods in Natural Language Processing*, pages 3824–3833, Brussels, Belgium. Association for Computational Linguistics.
- Bill Yuchen Lin, Xinyue Chen, Jamin Chen, and Xiang Ren. 2019. *KagNet: Knowledge-aware graph networks for commonsense reasoning*. In *Proceedings of the 2019 Conference on Empirical Methods in Natural Language Processing and the 9th International Joint Conference on Natural Language Processing (EMNLP-IJCNLP)*, pages 2829–2839, Hong Kong, China. Association for Computational Linguistics.
- Bing Liu and Ian Lane. 2016. *Attention-Based Recurrent Neural Network Models for Joint Intent Detection and Slot Filling*. In *Proc. Interspeech 2016*, pages 685–689.
- Yijin Liu, Fandong Meng, Jinchao Zhang, Jie Zhou, Yufeng Chen, and Jinan Xu. 2019a. *CM-net: A novel collaborative memory network for spoken language understanding*. In *Proceedings of the 2019 Conference on Empirical Methods in Natural Language Processing and the 9th International Joint Conference on Natural Language Processing (EMNLP-IJCNLP)*, pages 1051–1060, Hong Kong, China. Association for Computational Linguistics.
- Yinhan Liu, Myle Ott, Naman Goyal, Jingfei Du, Mandar Joshi, Danqi Chen, Omer Levy, Mike Lewis, Luke Zettlemoyer, and Veselin Stoyanov. 2019b. Roberta: A robustly optimized bert pretraining approach. *arXiv preprint arXiv:1907.11692*.
- Ilya Loshchilov and Frank Hutter. 2019. *Decoupled weight decay regularization*. In *ICLR*.
- Jinjie Ni, Tom Young, Vlad Pandelea, Fuzhao Xue, Vinay Adiga, and Erik Cambria. 2021. *Recent advances in deep learning based dialogue systems: A systematic survey*. *arXiv preprint arXiv:2105.04387*.
- Libo Qin, Wanxiang Che, Yangming Li, Haoyang Wen, and Ting Liu. 2019. *A stack-propagation framework with token-level intent detection for spoken language understanding*. In *Proceedings of the 2019 Conference on Empirical Methods in Natural Language Processing and the 9th International Joint Conference on Natural Language Processing (EMNLP-IJCNLP)*, pages 2078–2087, Hong Kong, China. Association for Computational Linguistics.
- Libo Qin, Zhouyang Li, Wanxiang Che, Minheng Ni, and Ting Liu. 2021a. *Co-gat: A co-interactive graph attention network for joint dialog act recognition and sentiment classification*. In *Proceedings of the AAAI Conference on Artificial Intelligence*, volume 35, pages 13709–13717.
- Libo Qin, Tailu Liu, Wanxiang Che, Bingbing Kang, Sendong Zhao, and Ting Liu. 2021b. *A co-interactive transformer for joint slot filling and intent detection*. In *ICASSP 2021 - 2021 IEEE International Conference on Acoustics, Speech and Signal Processing (ICASSP)*, pages 8193–8197.
- Libo Qin, Fuxuan Wei, Tianbao Xie, Xiao Xu, Wanxiang Che, and Ting Liu. 2021c. *GL-GIN: Fast and accurate non-autoregressive model for joint multiple intent detection and slot filling*. In *Proceedings of the 59th Annual Meeting of the Association for Computational Linguistics and the 11th International Joint Conference on Natural Language Processing (Volume 1: Long Papers)*, pages 178–188, Online. Association for Computational Linguistics.
- Libo Qin, Xiao Xu, Wanxiang Che, and Ting Liu. 2020. *AGIF: An adaptive graph-interactive framework for joint multiple intent detection and slot filling*. In *Findings of the Association for Computational Linguistics: EMNLP 2020*, pages 1807–1816, Online. Association for Computational Linguistics.
- Michael Sejr Schlichtkrull, Thomas N. Kipf, Peter Bloem, Rianne van den Berg, Ivan Titov, and Max Welling. 2018. *Modeling relational data with graph convolutional networks*. In *ESWC*, pages 593–607.
- Gokhan Tur and Renato De Mori. 2011. *Spoken language understanding: Systems for extracting semantic information from speech*. John Wiley & Sons.

- Laurens van der Maaten and Geoffrey Hinton. 2008. [Visualizing data using t-sne](#). *Journal of Machine Learning Research*, 9(86):2579–2605.
- Ashish Vaswani, Yonatan Bisk, Kenji Sagae, and Ryan Musa. 2016. [Supertagging with LSTMs](#). In *Proceedings of the 2016 Conference of the North American Chapter of the Association for Computational Linguistics: Human Language Technologies*, pages 232–237, San Diego, California. Association for Computational Linguistics.
- Ashish Vaswani, Noam Shazeer, Niki Parmar, Jakob Uszkoreit, Llion Jones, Aidan N. Gomez, Łukasz Kaiser, and Illia Polosukhin. 2017. [Attention is all you need](#). In *Advances in Neural Information Processing Systems 30: Annual Conference on Neural Information Processing Systems 2017, December 4-9, 2017, Long Beach, CA, USA*, pages 5998–6008.
- Petar Veličković, Guillem Cucurull, Arantxa Casanova, Adriana Romero, Pietro Liò, and Yoshua Bengio. 2018. [Graph attention networks](#). In *6th International Conference on Learning Representations, ICLR 2018, Vancouver, BC, Canada, April 30 - May 3, 2018, Conference Track Proceedings*. OpenReview.net.
- Yu Wang, Yilin Shen, and Hongxia Jin. 2018. [A bi-model based RNN semantic frame parsing model for intent detection and slot filling](#). In *Proceedings of the 2018 Conference of the North American Chapter of the Association for Computational Linguistics: Human Language Technologies, Volume 2 (Short Papers)*, pages 309–314, New Orleans, Louisiana. Association for Computational Linguistics.
- Di Wu, Liang Ding, Fan Lu, and Jian Xie. 2020. [SlotRefine: A fast non-autoregressive model for joint intent detection and slot filling](#). In *Proceedings of the 2020 Conference on Empirical Methods in Natural Language Processing (EMNLP)*, pages 1932–1937, Online. Association for Computational Linguistics.
- Bowen Xing and Ivor Tsang. 2022a. [DARER: Dual-task temporal relational recurrent reasoning network for joint dialog sentiment classification and act recognition](#). In *Findings of the Association for Computational Linguistics: ACL 2022*, pages 3611–3621, Dublin, Ireland. Association for Computational Linguistics.
- Bowen Xing and Ivor Tsang. 2022b. [Dignet: Diving clues from local-global interactive graph for aspect-level sentiment classification](#). *arXiv preprint arXiv:2201.00989*.
- Bowen Xing and Ivor Tsang. 2022c. [Neural subgraph explorer: Reducing noisy information via target-oriented syntax graph pruning](#). In *Proceedings of the Thirty-First International Joint Conference on Artificial Intelligence, IJCAI-22*, pages 4425–4431.
- Bowen Xing and Ivor W Tsang. 2022d. [Out of context: A new clue for context modeling of aspect-based sentiment analysis](#). *Journal of Artificial Intelligence Research*, 74:627–659.
- Bowen Xing and Ivor W. Tsang. 2022e. [Understand me, if you refer to aspect knowledge: Knowledge-aware gated recurrent memory network](#). *IEEE Transactions on Emerging Topics in Computational Intelligence*, 6(5):1092–1102.
- Steve Young, Milica Gašić, Blaise Thomson, and Jason D. Williams. 2013. [Pomdp-based statistical spoken dialog systems: A review](#). *Proceedings of the IEEE*, 101(5):1160–1179.
- Chenwei Zhang, Yaliang Li, Nan Du, Wei Fan, and Philip Yu. 2019. [Joint slot filling and intent detection via capsule neural networks](#). In *Proceedings of the 57th Annual Meeting of the Association for Computational Linguistics*, pages 5259–5267, Florence, Italy. Association for Computational Linguistics.
- Xiaodong Zhang and Houfeng Wang. 2016. [A joint model of intent determination and slot filling for spoken language understanding](#). In *Proceedings of the Twenty-Fifth International Joint Conference on Artificial Intelligence, IJCAI 2016, New York, NY, USA, 9-15 July 2016*, pages 2993–2999. IJCAI/AAAI Press.
- Suncong Zheng, Feng Wang, Hongyun Bao, Yueming Hao, Peng Zhou, and Bo Xu. 2017. [Joint extraction of entities and relations based on a novel tagging scheme](#). In *Proceedings of the 55th Annual Meeting of the Association for Computational Linguistics (Volume 1: Long Papers)*, pages 1227–1236, Vancouver, Canada. Association for Computational Linguistics.

## A Experiment Results on Pre-trained Language Model

To explore the effect of the pre-trained language model, we use the pre-trained RoBERTa (Liu et al., 2019b) encoder<sup>1</sup> to replace the self-attentive encoder and RoBERTa is fin-tuned in the training process. For each word, its first subword’s hidden state at the last layer is taken as its word representation fed to the BiLSTMs in Sec. 4.3.1. We adopt AdamW (Loshchilov and Hutter, 2019) optimizer to train the model with its default configuration. Since our computation resources are limited, we did not conduct hyper-parameter searching for RoBERTa+ReLa-Net. Thus we use the same hyper-parameters for RoBERTa+ReLa-Net with ReLa-Net (LSTM).

Fig. 9 shows the results comparison of our ReLa-Net, AGIF, and GL-GIN as well as their variants

<sup>1</sup>We use the RoBERTa-base checkpoint publicly that is available on <https://huggingface.co/roberta-base>.

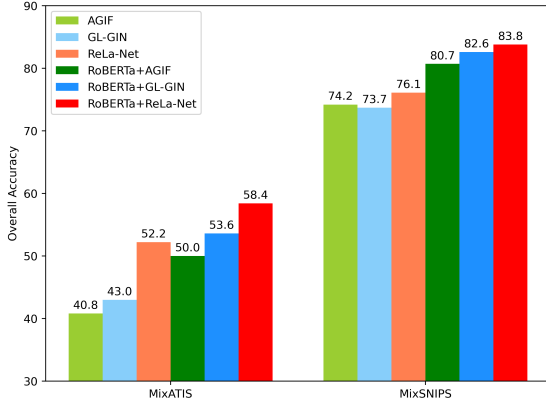


Figure 9: Overall accuracy comparison with RoBERTa.

using RoBERTa encoder. We have the following observations:

1. We can find that although the pre-trained RoBERTa encoder brings remarkable improvements via generating high-quality word representations, our RoBERTa+ReLa-Net significantly outperforms its counterparts. This is because the core of our ReLa-Net is capturing and leveraging the correlations among the intent labels and slot labels, which is not overlapped with the advantage of the pre-trained language model focusing on semantic features.
2. Although RoBERTa provides much better word representations, the performances of RoBERTa-based models are still not very satisfactory, especially on MixATIS (lower than 60%). We think the difficulty is mainly caused by the large number of labels, e.g. there are more than 135 labels in MixATIS dataset. Besides, our ReLa-Net (with LSTM encoder) even surpasses RoBERTa+AGIF. This is because ReLa-Net can capture and leverage the beneficial correlations among the massive labels. And this proves that the idea of exploiting label topologies and relations proposed in this paper is a promising perspective for improving joint multiple intent detection and slot filling.